HHS Public Access

Author manuscript

Cell Rep. Author manuscript; available in PMC 2016 January 08.

Published in final edited form as:

Cell Rep. 2015 December 22; 13(11): 2470–2479. doi:10.1016/j.celrep.2015.11.046.

T cell intrinsic USP15 deficiency promotes excessive IFN-γ production and an immunosuppressive tumor microenvironment in MCA-induced fibrosarcoma

Qiang Zou[1,2], **Jin Jin**[2,4], **Yichuan Xiao**[2,5], **Xiaofei Zhou**[2], **Hongbo Hu**[2,6], **Xuhong Cheng**[2], **Nasser Kazimi**[2], **Stephen E Ullrich**[2,3], and **Shao-Cong Sun**[2,3,*]

[1]Shanghai Institute of Immunology, Department of Immunology and Microbiology, Shanghai Jiao Tong University School of Medicine, 280 South Chongqing Road, Shanghai 200025, China

[2]Department of Immunology, The University of Texas MD Anderson Cancer Center, 7455 Fannin Street, Box 902, Houston TX 77030, USA

[3]The University of Texas Graduate School of Biomedical Sciences, Houston, TX 77030, USA

[4]Life Sciences Institute, Zhejiang University, Hangzhou 310058, China

[5]Institute of Health Sciences, Shanghai Institutes for Biological Sciences, Chinese Academy of Sciences and Shanghai Jiao Tong University School of Medicine, Shanghai 200031, China

[6]State Key Laboratory of Biotherapy, West China Hospital, Si-Chuan University and Collaborative Innovation Center for Biotherapy, Chengdu, 610041, China

Abstract

USP15 is a deubiquitinase that negatively regulates activation of naïve $CD4^+$ T cells and generation of IFN-γ-producing T helper 1 (Th1) cells. USP15 deficiency in mice promotes antitumor T cell responses in a transplantable cancer model; however, it has remained unclear how deregulated T cell activation impacts primary tumor development during the prolonged interplay between tumors and the immune system. Here, we find that the USP15-deficient mice are hypersensitive to methylcholantrene (MCA)-induced fibrosarcomas. Excessive IFN-γ production in USP15-deficient mice promotes expression of the immunosuppressive molecule PD-L1 and the chemokine CXCL12, causing accumulation of T-bet^+ regulatory T cells and $CD11b^+Gr\text{-}1^+$ myeloid-derived suppressor cells at tumor site. Mixed bone marrow adoptive transfer studies

*Correspondence: S.-C. S. (ssun@mdanderson.org).

AUTHOR CONTRIBUTIONS

Q.Z. designed and performed the experiments, prepared the figures, and wrote the manuscript; J.J., Y.X., X.Z., H.H., X.C., and N.K contributed to the performance of the experiments; N.K. and S.E.U. were involved in collaboration on cancer model studies; and S.-C.S. supervised the work and wrote the manuscript.

COMPETING FINANCIAL INTERESTS

The authors declare no competing financial interests.

SUPPLEMENTAL INFORMATION

Supplemental information includes 6 figures and 1 table.

further reveals a T cell-intrinsic role for USP15 in regulating IFN-γ production and tumor development. These findings suggest that T cell intrinsic USP15 deficiency causes excessive production of IFN-γ, which promotes an immunosuppressive tumor microenvironment, during MCA-induced primary tumorigenesis.

Keywords

Tumor microenvironment; IFN-γ; USP15; T cells; immunosuppression

INTRODUCTION

Cancer development involves dynamic interactions between tumor cells and the immune system, and a hallmark of tumors is their ability to evade immune surveillance (Dunn et al., 2004; Schreiber et al., 2011). Despite the infiltration of tumor-specific effector T cells at tumor site, these immune cells are largely ineffective in suppressing tumor growth. A common mechanism of immune evasion for most tumors is the establishment of an immunosuppressive microenvironment, composed of infiltrating T cells and innate immune cells in addition to the proliferating tumor cells and tumor stroma is a (Gajewski et al., 2013; Radoja et al., 2000; Whiteside, 2008; Zou, 2005). Tumor cells produce immunosuppressive factors, such as the ligand of the co-inhibitory receptor PD1, PD-L1, which suppress effector T function and promote the expansion of regulatory T (Treg) cells (Gajewski et al., 2013; Whiteside, 2008). Tumor cells also secrete soluble factors, such as cytokines and chemokines, which mediate recruitment of Treg cells and myeloid-derived suppressor cells (MDSCs), thereby facilitating the establishment of the immunosuppressive tumor microenvironment (Kitamura et al., 2015). It has been thought that immune cells have paradoxical roles in regulating cancer development. While immune cells mediate cancer immune surveillance, they also contribute to the formation of tumor microenvironment and promote tumor growth (Grivennikov et al., 2010; Whiteside, 2008).

Interferon-γ (IFN-γ), produced by effector T cells and innate immune cells, is known as a cytokine that promotes innate and adaptive immune responses against microbial infections and tumor development (Dunn et al., 2006). IFN-γ regulates the differentiation and effector function of different types of immune cells and also inhibits the growth and survival of cancer cells (Zaidi and Merlino, 2011). However, the role of IFN-γ in regulating antitumor immunity appears to be complex and paradoxical, showing both anti- and pro-tumorigenic functions (Wilke et al., 2011; Zaidi et al., 2011; Zaidi and Merlino, 2011). The mechanism underlying the two faces of IFN-γ function in antitumor immunity is incompletely understood, but IFN-γ appears to have different functions during different stages of tumor development. While IFN-γ is important for cancer immune destruction during the elimination phase in the model of tumor immunoediting, IFN-γ also contributes to the subsequent cancer immune evasion by promoting expression of tolerant molecules, such as PD-L1 and indoleamin-2,3-dioxygenase 1 (IDO1), and recruitment of Treg cells to tumor microenvironment (Schreiber et al., 2011; Spranger et al., 2013).

T cells, particularly the IFN-γ-producing $CD4^+$ T helper 1 (Th1) and $CD8^+$ effector T cells, are key components of the immune system for tumor surveillance and destruction (Kennedy and Celis, 2008; Klebanoff et al., 2006). Under physiological conditions, T cell activation is subject to tight regulation by various negative factors, which prevents abnormal T cell responses and autoimmunity. We have recently identified a deubiquitinase, USP15, which functions as a negative regulator of T cell receptor (TCR) signaling in $CD4^+$ T cells. USP15 deficiency promotes the activation of naïve $CD4^+$ T cells and their subsequent differentiation into the IFN-γ-producing Th1 cells (Zou et al., 2014). Although USP15 does not have a cell-intrinsic role in regulating $CD8^+$ T cells, the USP15 deficiency also promotes $CD8^+$ T cell responses *in vivo*, likely due to stronger helper function of Th1 cells. Compared to wildtype control mice, the USP15-deficient mice mount stronger T cell responses to tumor growth in a transplantable melanoma model, emphasizing the role of T cells in antitumor immunity (Zou et al., 2014). However, since the development of primary tumors involves a long period of interplays between tumors and the immune system, it has remained unclear how the excessive and chronic production of IFN-γ by USP15-deficient T cells impacts the development of primary tumors. To address this question, we employed a well-characterized model of chemical-induced tumorigenesis: the methylcholantrene (MCA)-induced fibrosarcoma (Swann et al., 2008). Interestingly, the USP15 deficiency profoundly enhanced the incidence of MCA-induced fibrosarcoma, coupled with excessive production of IFN-γ and an IFN-γ-responsive gene signature in tumor microenvironment. We further demonstrated that the T cell-intrinsic IFN-γ hyper-production in USP15-deficient mice promoted formation of an immunosuppressive tumor microenvironment along with MCA-induced primary tumorigenesis.

RESULTS

IFN-γ-responsive gene signature in the *Usp15*$^{-/-}$ tumor microenvironment

To examine the role of USP15 in regulating primary tumor formation, we employed the MCA-induced fibrosarcoma model of chemically induced tumorigenesis. We treated the wildtype and *Usp15*$^{-/-}$ mice with different doses of MCA and monitored tumor formation for up to 200 days. At both low and high doses of MCA treatment, the *Usp15*$^{-/-}$ mice developed fibroscomas with a significantly higher incidence compared to wildtype mice (Figure 1A). The *Usp15*$^{-/-}$ mice also had a more rapid onset of tumor formation than the wildtype control mice (Figure 1A). These results demonstrate that the *Usp15*$^{-/-}$ mice are more sensitive to the formation of MCA-induced fibrosarcomas.

To assess the mechanism by which USP15 regulates MCA-induced tumorigenesis, we analyzed the concentration of several major cytokines in the serum of the MCA-treated mice. While the wildtype and *Usp15*$^{-/-}$ mice had comparable levels of most serum cytokines analyzed, the *Usp15*$^{-/-}$ mice displayed a profound increase in the level of serum IFN-γ when treated with both low and high doses MCA (Figure 1B). A hallmark of tumors is the establishment of an immunosuppressive microenvironment, thereby evading immune surveillance (Gajewski et al., 2013; Whiteside, 2008). Although IFN-γ is generally considered as an antitumor immune mediator, it also induces the expression of immunosuppressive genes in tumor microenvironment (Zaidi and Merlino, 2011). Because

of the excessive production of IFN-γ in *Usp15*$^{-/-}$ mice, we performed quantitative reverse transcription polymerase chain reaction (qRT-PCR) assays to analyze gene expression in the CD45^{-} cell population, including tumor cells and other non-immune cells, of the MCA-induced tumors. Interestingly, the CD45^{-} cells of the *Usp15*$^{-/-}$ tumors displayed elevated expression of an IFN-γ-responsive gene signature (*Tbx21*, *Pd-l1*, *Irf1*, *Ido1*, *Cxcl5* and *Cxcl12*), most strikingly *Pd-l1* and *Cxcl12*, whereas the expression of IL-4 responsive genes (*Gata3* and *Ccl24*) was comparable between wildtype and *Usp15*$^{-/-}$ CD45^{-} cells (Figure 1C). The elevated expression of PD-L1 and CXCL12 in the *Usp15*$^{-/-}$ CD45^{-} cells was also detected at the level of protein by flow cytometry assays (Figure 1D and 1E).

To determine the functional significance of the aberrant expression of PD-L1 and CXCL12 in promoting MCA-induced tumor development in *Usp15*$^{-/-}$ mice, we injected the MCA-challenged mice with neutralizing antibodies for PD-LI or CXCL12. The PD-L1 antibody significantly reduced the incidence of MCA-induced tumors in both wildtype and *Usp15*$^{-/-}$ mice (Figure 1F and Figure S1). However, this phenotype was much more striking for the *Usp15*$^{-/-}$ mice, consistent with the elevated PD-L1 expression in the tumor microenvironment of these mutant mice. Treatment of the *Usp15*$^{-/-}$ mice with the anti-CXCL12 antibody also reduced the tumor incidence (Figure 1G). These data suggest that altered tumor microenvironment, including aberrant expression of PD-L1 and the chemokine CXCL12, contributes to the enhanced tumorigenesis in MCA-treated *Usp15*$^{-/-}$ mice.

Accumulation of T-bet^{+} Treg cells in tumor microenvironment of *Usp15*$^{-/-}$ mice

Foxp3^{+}CD4^{+} Treg cells promote tumor formation and progression by inhibiting antitumor responses and mediating tumor immune escape (Zou, 2006). To further elucidate the mechanism by which USP15 regulates MCA-induced primary tumorigenesis, we analyzed the abundance and function of Treg cells at the tumor site of wildtype and *Usp15*$^{-/-}$ mice. Under tumor-free conditions (injected with solvent control), the wildtype and *Usp15*$^{-/-}$ mice had a similar frequency of Treg cells in the draining lymph node (Figure S2A). However, the tumor-bearing *Usp15*$^{-/-}$ mice had a significantly higher frequency and absolute number of Treg cells than the wildtype mice in both the tumor and draining lymph node (Figure 2A and Figure S2B). This phenotype was not seen in the spleen, in which the wildtype and mutant mice had comparable levels of Treg cells (Figure S2C), suggesting increased recruitment or generation of Treg cells at tumor site of the *Usp15*$^{-/-}$ mice.

We noted that tumor-infiltrating Treg cells expressed a higher level of CXCR4 than splenic Treg cells in both wildtype and *Usp15*$^{-/-}$ mice (Figure 2B). CXCR4 is a receptor of the chemokine CXCL12, which has been implicated in the regulation of Treg cell recruitment to the tumor site (Durr et al., 2010). Because of the elevated expression of CXCL12 in *Usp15*$^{-/-}$ tumor microenvironment (Figure 1C and 1E), we examined the possible involvement of the CXCL12/CXCR4 axis in Treg accumulation in the tumor microenvironment of *Usp15*$^{-/-}$ mice. Antibody-mediated CXCL12 blockade reduced the frequency and absolute numbers of Treg cells in the tumor of *Usp15*$^{-/-}$ mice (Figure 2C). These results suggest that deregulated expression of the chemokine CXCL12 contributes to the abnormal Treg cell accumulation at the tumor site of *Usp15*$^{-/-}$ mice.

Recent evidence suggests that Treg cells display dynamic expression of the transcription factors T-bet and GATA-3, which are important for Treg-mediated immune tolerance (Yu et al., 2015). Of note, the expression of T-bet and GATA-3 can be stimulated by IFN-γ and IL-4, respectively. We found that Treg cells from the tumor and tumor-draining lymph node of *Usp15*$^{-/-}$ mice expressed a higher level of T-bet, although not GATA3, than the Treg cells from wildtype mice (Figure 2D, Figure S2D and data not shown). This phenotype appeared to be specific for tumor microenvironment, since splenic Treg cells of the *Usp15*$^{-/-}$ and wildtype mice had a comparable level of T-bet (Figure S2D). The USP15 deficiency did not alter the sensitivity of Treg cells to IFN-γ-induced T-bet expression, suggesting that excessive IFN-γ production contributed to the enhanced T-bet^{+} Treg cells in *Usp15*$^{-/-}$ tumor environment (Figure 2E).

We next examined the immunosuppressive function of the USP15-deficient Treg cells using an *in vivo* model involving inoculation of the T cell-deficient *Tcrb*$^{-/-}$*Tcrd*$^{-/-}$ mice with OVA-expressing B16 melanoma cells and subsequent adoptive transfer of the OVA-specific OT-I T cells along with either wildtype or USP15-deficient Treg cells from tumor-bearing or naïve mice. Overall, the Treg cells derived from tumor-bearing mice displayed stronger suppressive function than those derived from naïve mice (Figure 2F). Furthermore, while the wildtype and USP15-deficient Treg cells from naïve mice displayed similar levels of suppressive function, the USP15-deficient Treg cells were significantly more suppressive than the wildtype Treg cells when they were isolated from tumor-bearing mice (Figure 2F). These results were consistent with the upregulated T-bet expression in *Usp15*$^{-/-}$ Treg cells under tumor-bearing conditions (Figure 2D). The Treg cells from USP15-deficient tumor-bearing mice also more potently inhibited the proliferation of native T cells *in vitro* than Treg cells from wildtype tumor-bearing mice (Figure 2G). Moreover, Treg cell down-regulation by a neutralizing anti-CD25 antibody significantly reduced the incidence of tumor formation in *Usp15*$^{-/-}$ mice (Figure 2H), whereas the anti-CD25 antibody only slightly decreased the incidence of MCA-induced tumors in wildtype mice (Figure S2E). Taken together, these results suggest that recruitment and induction of T-bet^{+} Treg cells contributes to the enhanced tumor formation in *Usp15*$^{-/-}$ mice.

USP15 regulates MDSC recruitment to tumor environment

In addition to Treg cells, MDSCs, characterized by high levels of surface Gr-1 and CD11b, play an important role in maintaining immunosuppressive tumor microenvironment and promoting tumor growth (Nagaraj and Gabrilovich, 2008). MDSC expansion and recruitment to tumor site are induced by inflammatory cytokines and chemokines secreted by immune cells and tumor cells (Gabrilovich and Nagaraj, 2009; Ostrand-Rosenberg and Sinha, 2009; Umansky and Sevko, 2013). In particular, both IFN-γ and the chemokine CXCL12 have been implicated in the induction of MDSC accumulation in tumor tissues (Umansky and Sevko, 2013). Because of the excessive production of IFN-γ by T cells and upregulation of CXCL12 in tumor tissues of the *Usp15*$^{-/-}$ mice, we analyzed the abundance of MDSCs at the tumor site of wildtype and *Usp15*$^{-/-}$ mice. The tumor tissue of *Usp15*$^{-/-}$ mice contained a profoundly higher frequency and number of the Gr-1^{+}CD11b^{+} MDSCs than the tumor tissue of the wildtype mice (Figure 3A and 3B). Similarly, a significant

increase in the frequency and number of MDSCs was detected in the tumor-draining lymph node, although not in the spleen, of *Usp15*$^{-/-}$ mice (Figure 3B and Figure S2F and S2G).

The tumor-infiltrating MDSCs (Gr-1^{+}CD11b^{+} cells) of both the wildtype and *Usp15*$^{-/-}$ mice expressed high levels of the CXCL12 receptor, CXCR4 (Figure 3C). Because of the elevated expression of CXCL12 in the tumor of *Usp15*$^{-/-}$ mice, we examined the role of CXCL12 in mediating MDSC recruitment to tumor site. Indeed, injection of the tumor-bearing *Usp15*$^{-/-}$ mice with a CXCL12-neutralizing antibody, but not a control antibody, substantially reduced the frequency and absolute number of MDSCs in the tumor (Figure 3D). These data suggest that aberrant production of the chemokine CXCL12 contributes to the accumulation of tumor-infiltrating MDSCs in the *Usp15*$^{-/-}$ mice.

Since MDSCs have been implicated to suppress the antitumor function of T cells (Umansky and Sevko, 2013), we compared the immunosuppressive function of the MDSCs (Gr-1^{+}CD11b^{+} cells) derived from tumor-bearing wildtype and *Usp15*$^{-/-}$ mice. We used an adoptive transfer model involving injection of T cell-deficient (*Tcrb*$^{-/-}$*Tcrd*$^{-/-}$) mice with OVA-expressing B16 melanoma cells and subsequent transfer of OVA-specific OT-I T cells along with sorted Gr-1^{+}CD11b^{+} cells. As expected, OT-I T cells efficiently inhibited B16 tumor growth in the absence of MDSCs (Figure 3E). Furthermore, MDSCs derived from wildtype and the USP15-deficient mice displayed similar activities in suppressing the tumor-rejecting function of OT-I T cells (Figure 3E). In an *in vitro* model of T cell proliferation assay, the wildtype and USP15-deficient MDSCs also displayed similar T cell-inhibitory function (Figure 3F). Thus, USP15 deficiency promotes the accumulation of MDSCs, although it does not alter the T cell-suppressive activity of MDSCs.

IFN-γ blockade disrupts the immunosuppressive tumor microenvironment

IFN-γ is generally viewed as a cytokine that mediates antitumor immunity, but it also has pro-tumorigenic functions (Zaidi et al., 2011; Zaidi and Merlino, 2011). It has remained unclear how excessive production of IFN-γ impacts tumor microenvironment during MCA-induced tumorigenesis. We determined the role of IFN-γ in establishing the immunosuppressive tumor microenvironment of *Usp15*$^{-/-}$ mice by administration of a neutralizing anti-IFN-γ antibody. Injection of the anti-IFN-γ antibody, but not a control IgG1 antibody, efficiently inhibited the expression of IFN-γ-associated gene signature, particularly *Pd-l1* and *Cxcl12*, in tumor tissues (Figure 4A). On the other hand, the anti-IFN-γ treatment did not alter the expression of several other genes, including those encoding the chemokines CCL1, CCL22, and CCL24 (Figure 4A). The IFN-γ neutralizing antibody also reduced the expression of PD-L1 and CXCL12 at the protein level (Figure 4B and 4C). Moreover, IFN-γ neutralization reduced the frequency and number of tumor-infiltrating Treg cells (Figure 4D) and inhibited T-bet expression in Treg cells (Figure 4E). The abnormal Gr-1^{+}CD11b^{+} cell recruitment was also reversed in the presence of the IFN-γ neutralizing antibody (Figure 4F). The IFN-γ blockade also delayed the formation of MCA-induced fibrosarcomas in the *Usp15*$^{-/-}$ mice (Figure 4G). Compared to anti-PD-L1 and anti-CD25, the anti-IFN-γ antibody was less effective in tumor inhibition. This result was likely due to the duel roles for IFN-γ in regulating antitumor immunity (Zaidi and Merlino, 2011).

Notwithstanding, these data reveal an essential role for aberrant IFN-γ signaling in promoting immunosuppressive microenvironment formation.

T cells are major source of aberrant IFN-γ production in *Usp15*$^{-/-}$ mice

IFN-γ is an inflammatory cytokine produced by Th1 subset of CD4$^+$ T cells and CD8$^+$ T cells as well as by some innate immune cells, including natural killer (NK) cells and macrophages (Gessani and Belardelli, 1998; Kubota, 2010; Schoenborn and Wilson, 2007). To determine the source of the aberrantly higher level of serum IFN-γ in *Usp15*$^{-/-}$ mice, we examined whether the USP15 deficiency promoted IFN-γ production in T cells or innate immune cells at the tumor site. In the spleen, the frequency and absolute numbers of the IFN-γ-producing Th1 and CD8$^+$ T cells, as well as other T cell subsets, were similar between wildtype and *Usp15*$^{-/-}$ mice (Figure S3A and S3B). However, in the tumor-draining lymph node, the *Usp15*$^{-/-}$ mice had a significantly higher frequency and absolute number of IFN-γ-producing CD4$^+$ and CD8$^+$ T cells, whereas the frequency and absolute number of IL-4-producing Th2 and IL-17-producing Th17 cells were comparable between the wildtype and *Usp15*$^{-/-}$ mice (Figure 5A and 5B). Similarly, the tumor-infiltrating lymphocytes (TILs) of *Usp15*$^{-/-}$ mice contained a profoundly higher level of IFN-γ-producing Th1 and CD8$^+$ T cells (Figure 5C and 5D). Moreover, the aberrant activation of Th1 and CD8$^+$ T cells in the *Usp15*$^{-/-}$ mice was specifically caused by tumorigenesis, since the control (injected with oil) wildtype and *Usp15*$^{-/-}$ mice had similar frequency and absolute numbers of IFN-γ-producing CD4$^+$ or CD8$^+$ T cells in the draining lymph node (Figure S3C and S3D).

We next examined IFN-γ production in innate immune cells. Compared to splenic NK cells (CD3$^-$NK1.1$^+$), the tumor-infiltrating NK cells displayed a much higher level of *Ifng* gene expression, as determined by qRT-PCR assays (Figure 5E). However, this phenotype was seen in both wildtype and USP15-deficient NK cells. The wildtype and USP15-dericient NK cells were also comparable in IFN-γ expression upon *in vitro* stimulation with LPS (Figure 5F and 5G). Furthermore, USP15 deficiency also did not influence *Ifng* expression in tumor-infiltrating or splenic macrophages (F4/80$^+$CD11b$^+$) (Figure 5E). Since dendritic cells are important for T-cell activation in antitumor immune responses, we next performed experiments to compare the T-cell stimulating function of wildtype and *Usp15*$^{-/-}$ DCs. The wildtype and *Usp15*$^{-/-}$ DCs, derived from the lymph nodes of naïve or tumor-bearing mice, did not show major differences in their capacity to stimulate naïve T cell proliferation (Figure S3E). Moreover, DCs from wildtype and *Usp15*$^{-/-}$ tumor-bearing mice exhibited similar levels of type I interferon expression (Figure 5H). These results further emphasize the role of USP15 in regulating IFN-γ expression in T cells.

USP15-deficient T cells promotes MCA-induced tumorigenesis

Because of the association of aberrantly activated T cells with enhanced tumorgenesis in the *Usp15*$^{-/-}$ mice, we performed mixed bone marrow adoptive transfer studies to directly examine the T cell-specific role of USP15 in regulating MCA-induced fibrosarcoma. We adoptively transferred the lymphocyte-deficient *Rag1*$^{-/-}$ mice with a mixture of bone marrow cells derived from *Usp15*$^{-/-}$ and *Tcrb*$^{-/-}$*Tcrd*$^{-/-}$ mice, and then challenged the recipient mice (hereafter called *Usp15*$^{-/-}$ chimeric mice) with MCA (Figure 6A). Since the

Tcrb$^{-/-}$*Tcrd*$^{-/-}$ bone marrow could generate all immune cells, except T cells, the *Usp15*$^{-/-}$ chimeric mice would contain USP15-deficient T cells and wildtype innate immune cells, B cells, and non-immune cells (including the tumor cells). As controls, we generated bone marrow chimeric mice by transferring a mixture of wildtype bone marrow and *Tcrb*$^{-/-}$*Tcrd*$^{-/-}$ bone marrow (hereafter called wildtype chimeric mice). Under these conditions, the *Usp15*$^{-/-}$ chimeric mice were substantially more sensitive to MCA-induced tumorigenesis than the wildtype chimeric mice, as shown by both tumor incidence and tumor growth rate (Figure 6B and 6C). As seen with *Usp15*$^{-/-}$ mice (Figure 1B), the *Usp15*$^{-/-}$ chimeric mice had a significantly higher level of serum IFN-γ than that of the control chimeric mice (Figure 6D). Furthermore, the *Usp15*$^{-/-}$ chimeric mice had a greater level of IFN-γ-producing CD4^{+} and CD8^{+} T cells than wildtype chimeric mice in the draining lymph nodes and tumor tissues, although not in the spleen (Figure 6E and 6F; Figure S4A). The level of other T-cell subsets was comparable between the *Usp15*$^{-/-}$ and wildtype chimeric mice (Figure S4B and S4C). These results were reminiscent of those obtained with the *Usp15*$^{-/-}$ mice, thus suggesting a T cell-intrinsic role for USP15 in regulating MCA-induced T-cell function and primary tumor formation.

USP15-deficient T cells contribute to immunosuppressive tumor microenvironment

To further assess the mechanism underlying the T cell-intrinsic role of USP15 in regulating MCA-induced tumorigenesis, we analyzed the effect of USP15 deficiency on the formation of immunosuppressive tumor microenvironment using the mixed bone marrow chimeric mice described above. The tumor of the *Usp15*$^{-/-}$ chimeric mice had upregulated expression of PD-L1 and CXCL12 (Figures 7A–7C). These chimeric mice also had a higher frequency and absolute number of Foxp3^{+}CD4^{+} Treg cells in the draining lymph node and tumor, although not in the spleen (Figures 7D and 7E, Figure S5A). As seen with the *Usp15*$^{-/-}$ mice, the USP15-deficient Treg cells derived from the *Usp15*$^{-/-}$ chimeric mice had an elevated level of T-bet expression (Figure 7F). Moreover, the *Usp15*$^{-/-}$ chimeric mice displayed a higher percentage and absolute number of MDSCs in the tumor, draining lymph node, but not in the spleen, compared to the wildtype chimeric mice (Figure 7G and Figure S5B). Together, these adoptive transfer experiments suggest a T cell-intrinsic role for USP15 deficiency in promoting IFN-γ production and immunosuppressive tumor microenvironment formation.

USP15 deficiency promotes immunity against transplanted MCA tumors

Our previous work demonstrates that USP15 deficiency promotes antitumor immunity in a transplantable B16 melanoma tumor model (Zou et al., 2014), which differs from the present findings obtained using the MCA-induced primary tumor model. This result is, however, not surprising, since transplantable tumors bypass the cellular transformation phase of tumorigenesis and trigger acute antitumor immune responses without involving a long period of tumor-immune system interactions. However, it is also possible that USP15 may have opposing roles in immune responses against different types of tumors. To examine these possibilities, we employed a transplantable tumor model using a tumor cell line derived from the MCA-induced fibrosarcoma, MCA-205. As seen with the B16 melanoma model, USP15 deficiency enhanced host defense against the transplanted MCA tumors, leading to significantly smaller tumors in the *Usp15*$^{-/-}$ mice than in the wildtype mice

(Figure S6A). Consistently, the *Usp15*$^{-/-}$ mice had increased frequency and absolute number of IFN-γ-producing T cells infiltrating to the tumors (Figure S6B). Likely due to the acute nature of the antitumor immunity in the transplantable tumor model, the stronger T-cell response did not substantially alter the immunosuppressive cell populations, since the MCA-205 tumors in wildtype and *Usp15*$^{-/-}$ mice had similar frequency and absolute number of tumor-infiltrating Treg cells and MDSCs (Figures S6C and S6D). The wildtype and USP15-deficient Treg cells also expressed similar levels of T-bet (Figures S6E). These findings indicate that USP15 ablation promotes immunity against transplantable MCA-205, as well as B16, tumors.

DISCUSSION

Cancer development involves dynamic interplays between tumor and the immune system, with the immune system possessing paradoxical functions (de Visser et al., 2006; Whiteside, 2008). Although the anti-tumorigenic function of the immune system has been extensively studied, the pro-tumorigenic function of immune cells has been incompletely understood. In particular, whether chronic and excessive activation of IFN-γ-producing T cells inhibits or promotes tumorigenesis is incompletely understood. In the present study, we demonstrated that ablation of the T cell negative regulator, USP15, caused hyper-activation of IFN-γ-secreting T cells and increased the incidence of primary tumor formation in the MCA fibrosarcoma primary tumor model. The USP15-deficient T cells, likely via excessive production of IFN-γ, promoted an immunosuppressive tumor microenvironment that suppressed antitumor immunity.

IFN-γ is generally viewed as an inflammatory cytokine that promotes cellular immunity against infections and tumor development; however, accumulating evidence implicates IFN-γ as a cytokine with both anti- and pro-tumorigenic functions (Zaidi and Merlino, 2011). We have previously shown that the *Usp15*$^{-/-}$ mice mount stronger IFN-γ^{+} T cell responses and antitumor immunity than wildtype control mice in a transplantable B16 melanoma model (Zou et al., 2014). Our present study further demonstrated excessive IFN-γ^{+} T cell responses of the *Usp15*$^{-/-}$ mice during MCA-induced primary fibrosarcoma development. However, in contrast to their enhanced ability to reject transplantable tumors, the *Usp15*$^{-/-}$ mice were more sensitive to MCA-induced tumor formation. These opposing results were not due to the differences between melanoma and fibrosarcoma, since the *Usp15*$^{-/-}$ mice also had stronger ability to reject transplanted MCA-205 tumors than wildtype mice. We believe that the seemingly controversial results are likely due to the major differences in the formation of primary and transplantable tumors (Dranoff, 2012). In particular, formation of transplantable tumors bypasses the early steps of tumorigenesis. Although this model is ideal for studying antitumor immunity against pre-established tumors, it is unable to study the effect of immune system on the early steps of tumor development, which typically involves dynamic interplays between tumors and the immune system and establishment of a complex tumor microenvironment (Schreiber et al., 2011; Whiteside, 2008; Zou, 2005). Differences between primary and transplantable tumor models have also been seen with other mouse models, such as mice lacking the innate immune signaling adaptor MyD88 (Swann et al., 2008).

Our present study revealed that in the MCA-induced fibrosarcoma model, USP15 deficiency caused hyper-activation of IFN-γ^+ T cells, which was associated with formation of a more immunosuppressive tumor microenvironment characterized by upregulated expression of PD-L1 and CXCL12 and enhanced recruitment of Treg cells and MDSCs. Such phenotypes could be reversed by downregulation of IFN-γ function with a neutralizing anti-IFN-γ antibody. These findings suggest that although USP15 deficiency promotes antitumor T cell responses against pre-established (transplanted) tumors, the chronic production of excessive IFN-γ in *Usp15*$^{-/-}$ mice may promote primary tumor development through facilitating the establishment of immunosuppressive tumor microenvironment. Mixed bone marrow adoptive transfer experiments confirmed the T cell-intrinsic function of USP15 in regulating IFN-γ production and tumor microenvironment formation, emphasizing a protumorigenic role for T cell-derived IFN-γ. However, it is important to note that our data could not rule out the possibility that the function of USP15 in regulating tumor microenvironment also involves additional mechanisms. Nevertheless, the excessive production of IFN-γ in *Usp15*$^{-/-}$ mice appears to be one factor that contributes to the establishment or maintenance of immunosuppressive tumor microenvironment in the MCA fibrosarcoma model of tumorigenesis.

Treg cells and MDSCs are major cellular components in the tumor microenvironment that inhibit antitumor immune responses (Gajewski et al., 2013; Umansky and Sevko, 2013; Whiteside, 2008). Our data suggest that the chemokine CXCL12 was responsible for enhanced recruitment of Treg cells and MDSCs to tumor site in *Usp15*$^{-/-}$ mice. CXCL12 was upregulated in the tumor microenvironment of *Usp15*$^{-/-}$ mice in an IFN-γ-dependent manner, and antibody-mediated CXCL12 neutralization reduced the frequency of Treg cells and MDSCs at tumor site. The excessive production of IFN-γ in *Usp15*$^{-/-}$ mice also promoted the effector function of Treg cells, which involved induction of the transcription factor T-bet. The T-bet$^+$ Treg cells are known to be important for controlling the function of Th1 cells and, thereby, suppressing Th1 cell-mediated inflammatory responses (Hall et al., 2012; Koch et al., 2012; Koch et al., 2009). Our data suggest that these Treg cells also potently suppress the effector function of CD8$^+$ T cells in antitumor immunity. The accumulation of T-bet$^+$ Treg cells in the tumor of *Usp15*$^{-/-}$ mice was caused by loss of USP15 in T cells and apparently due to the aberrant expression of IFN-γ.

In summary, the present study confirmed our previous finding that USP15 negatively regulates T cell responses to tumor formation (Zou et al., 2014). However, the USP15-mediated T cell regulation appears to have different roles in antitumor immunity. On the one hand, USP15 deficiency enhances the ability of T cells to reject pre-established tumors, as suggested by work with transplantable tumor models (Zou et al., 2014 and present study). On the other hand, the aberrant activation of the USP15-deficient T cells appears to promote an immunosuppressive tumor microenvironment that facilitates tumor development during the long period of tumor-immune system interplay. It is thus possible that inhibition of USP15, along with targeting immunosuppressive regulators of the tumor microenvironment, may induce strong antitumor immunity. While this possibility needs to be examined by future studied, we have shown that in the MCA-induced fibrosarcoma model, neutralizing

antibodies for PD-L1 and CXCL12 inhibit tumor formation more effectively in *Usp15*$^{-/-}$ mice than in wildtype mice.

EXPERIMENTAL PROCEDURES

Mice

Usp15$^{-/-}$ mice were generated using the OmniBank retroviral gene-trapping technique (Taconic). The mice were originally in C57BL/6-129 mixed background and subsequently backcrossed for six generations to the C57BL/6 background. Heterozygous (*Usp15*$^{+/-}$) mice were bred to generate age-matched wildtype (*Usp15*$^{+/+}$) and homozygous *Usp15*-KO (*Usp15*$^{-/-}$) experimental mice. *Tcrb*$^{-/-}$*Tcrd*$^{-/-}$ mice, *Rag1*$^{-/-}$ mice and OT-I TCR-transgenic mice were obtained from Jackson Laboratory. Mice were maintained in specific pathogen-free facility, and all animal experiments were conducted in accordance with protocols approved by the Institutional Animal Care and Use Committee of the University of Texas MD Anderson Cancer Center.

Antibodies, reagents and cell lines

PE-conjugated anti-mouse CD274 (PD-L1, B7-H1) and other additional antibodies for flow cytometry were from eBioscience as described. Mouse CXCL12 (clone: 79014) neutralizing antibody was from R&D systems. Rat anti-mouse IFN-γ (clone: XMG1.2), rat IgG1 isotype control (clone: HRPN), rat anti-mouse CD25 (clone: PC-61.5.3), rat anti-mouse PD-L1 (clone: 10F.9G2), rat IgG2b isotype control (clone: LTF-2) and mouse IgG1 isotype control (clone: MOPC-21) antibodies were from Bioxcell. 3-Methylcholanthrene (MCA) was from Sigma-Aldrich. MCA-205 cell line was kindly provided by Dr. Tomasz Zal (MD Anderson Cancer Center, TX).

MCA-induced fibrosarcoma

Induction of fibrosarcoma using the carcinogen MCA was essentially as described (Swann et al., 2008). Wildtype and *Usp15*$^{-/-}$ mice were given subcutaneous injection of low or high doses of MCA (400 μg or 800 μg), as indicated in the figure legends, on the right flank. The mice were monitored for the development of fibrosarcomas weekly over the course of 200 days. Tumor size was presented as a caliper square calculated based on 2 perpendicular diameters (mm^2). Mice with tumors larger than 225 mm^2 were sacrificed and recorded as lethal based on protocols approved by the Institutional Animal Care and Use Committee of the University of Texas MD Anderson.

Isolation of TIL

Tumors were pressed and collected in complete RPMI 1640. After washing (300 × *g*, 10 min), cell suspensions were resuspended in complete RPMI 1640 containing collagenase IV (0.05%; Roche Applied Science, Indianapolis, IN) at 37°C for 30 to 40 min. After digestion, cell suspensions were passed through 70-μm nylon cell strainers to yield single-cell suspensions. $CD45^+$ cells (TILs) were sorted for further analysis.

Flow cytometry analysis

Single cell suspensions were made from spleens, draining lymph nodes and tumor tissues. These cells were stained with indicated specific conjugated antibodies and subjected to flow cytometry, and cell sorting as described using LSR II (BD Bioscience) and FACSAria (BD Bioscience) flow cytometers, respectively. For ICS, single cell suspensions were further stimulated for 4 h with PMA plus ionomycin in the presence of monensin and then subjected to intracellular staining and flow cytometry. The data were analyzed using FlowJo software.

ELISA and quantitative RT-PCR

Serum was collected from the mice and then was analyzed by ELISA using a commercial assay system (eBioscience). Total RNA was extracted from sorted $CD45^-$ cells from the tumor tissues. cDNA was synthesized and then subjected to qRT-PCR using gene-specific primers (Table S1).

Antibody-mediated neutralization

Mice were injected i.p. with 500 μg PD-L1 (clone: 10F.9G2), 100 μg CXCL12 (clone: 79014), 500 μg CD25 (clone: PC-61.5.3) or 500 μg IFN-γ (clone: XMG1.2) neutralizing antibodies. Injections were performed once a week for 8 weeks from day 90 to day 146 after MCA injection. Control groups in PD-L1 neutralization experiments received rat IgG2b (clone: LTF-2); controls for CXCL12 neutralization experiments received mouse IgG1 (clone: MOPC-21), whereas controls in CD25 and IFN-γ neutralization experiments received rat IgG1 isotype control (clone: HRPN).

Adoptive T cell immunotherapy model

Tcrb$^{-/-}$*Tcrd*$^{-/-}$ mice were injected s.c. with 2×10^5 B16 melanoma cells expressing a surrogate tumor antigen, OVA. At day 6 after tumor injection, mice received an i.v. injection of PBS control, 1×10^6 OT-I $CD8^+$ T cells, 1×10^6 OT-I $CD8^+$ T cells plus 2×10^5 $CD4^+CD25^+$ T cells (Treg), or 1×10^6 OT-I $CD8^+$ T cells plus 2×10^5 Gr-1^+CD11b^+ cells (MDSC). The challenged mice were monitored for tumor growth. Splenic OT-I $CD8^+$ T cells were sorted from naïve OT-I mice. Treg cells and MDSCs were sorted from tumor-bearing wildtype and *Usp15*$^{-/-}$ mice.

T cell proliferation assays

Splenic OT-I $CD8^+$ T cells were sorted from naïve OT-I mice and labeled with 5μM CFSE for 10 min at 37°C. 5×10^4 CFSE-labeled T cells were co-cultured with 1.5×10^5 splenocytes from naïve B6 mice and $CD4^+CD25^+$ T cells (Treg) or Gr-1^+CD11b^+ cells (MDSC) from the tumor of tumor-bearing mice in the presence of 0.1μg $OVA_{257\text{-}264}$ peptide for 2 days. Cell proliferation was measured by flow cytometry based on CFSE dilution.

Adoptive transfer of bone marrow cells

Bone marrow cells (1×10^6) isolated from *Usp15*$^{-/-}$ or wild-type mice were mixed with bone marrow cells (4×10^6) from *Tcrb*$^{-/-}$*Tcrd*$^{-/-}$ mice (in 1:4 ratio) and adoptively transferred into irradiated (950 rad) *Rag 1*$^{-/-}$ mice.

Statistical analysis

Statistical analysis was performed using Prism software. Two-tailed unpaired *t*-tests were performed and *P* values less than 0.05 were considered significant, and the level of significance was indicated as $*P < 0.05$ and $**P < 0.01$. Differences in tumor incidence were evaluated with the Mantel-Cox test.

Supplementary Material

Refer to Web version on PubMed Central for supplementary material.

Acknowledgments

We thank Drs. Junmei Wang and Roza Nurieva for discussions and technical support in mouse tumor models and Dr. Tomasz Zal for providing MCA-205 cell line. We also thank the personnel from the NIH/NCI-supported resources (flow cytometry, DNA analysis, histology, and animal facilities) under award number P30CA016672 at The MD Anderson Cancer Center. This study was supported by grants from Cancer Prevention and Research Institute of Texas (RP140244) and National Institutes of Health (AI064639) and partially supported by a seed fund from the Center for Inflammation and Cancer at the MD Anderson Cancer Center.

References

de Visser KE, Eichten A, Coussens LM. Paradoxical roles of the immune system during cancer development. Nature reviews Cancer. 2006; 6:24–37. [PubMed: 16397525]

Dranoff G. Experimental mouse tumour models: what can be learnt about human cancer immunology? Nat Rev Immunol. 2012; 12:61–66. [PubMed: 22134155]

Dunn GP, Koebel CM, Schreiber RD. Interferons, immunity and cancer immunoediting. Nat Rev Immunol. 2006; 6:836–848. [PubMed: 17063185]

Dunn GP, Old LJ, Schreiber RD. The three Es of cancer immunoediting. Annu Rev Immunol. 2004; 22:329–360. [PubMed: 15032581]

Durr C, Pfeifer D, Claus R, Schmitt-Graeff A, Gerlach UV, Graeser R, Kruger S, Gerbitz A, Negrin RS, Finke J, Zeiser R. CXCL12 mediates immunosuppression in the lymphoma microenvironment after allogeneic transplantation of hematopoietic cells. Cancer Res. 2010; 70:10170–10181. [PubMed: 21159639]

Gabrilovich DI, Nagaraj S. Myeloid-derived suppressor cells as regulators of the immune system. Nat Rev Immunol. 2009; 9:162–174. [PubMed: 19197294]

Gajewski TF, Schreiber H, Fu YX. Innate and adaptive immune cells in the tumor microenvironment. Nat Immunol. 2013; 14:1014–1022. [PubMed: 24048123]

Gessani S, Belardelli F. IFN-gamma expression in macrophages and its possible biological significance. Cytokine Growth Factor Rev. 1998; 9:117–123. [PubMed: 9754706]

Grivennikov SI, Greten FR, Karin M. Immunity, inflammation, and cancer. Cell. 2010; 140:883–899. [PubMed: 20303878]

Hall AO, Beiting DP, Tato C, John B, Oldenhove G, Lombana CG, Pritchard GH, Silver JS, Bouladoux N, Stumhofer JS, et al. The cytokines interleukin 27 and interferon-gamma promote distinct Treg cell populations required to limit infection-induced pathology. Immunity. 2012; 37:511–523. [PubMed: 22981537]

Kennedy R, Celis E. Multiple roles for CD4+ T cells in anti-tumor immune responses. Immunol Rev. 2008; 222:129–144. [PubMed: 18363998]

Kitamura T, Qian BZ, Pollard JW. Immune cell promotion of metastasis. Nat Rev Immunol. 2015; 15:73–86. [PubMed: 25614318]

Klebanoff CA, Gattinoni L, Restifo NP. CD8+ T-cell memory in tumor immunology and immunotherapy. Immunol Rev. 2006; 211:214–224. [PubMed: 16824130]

Koch MA, Thomas KR, Perdue NR, Smigiel KS, Srivastava S, Campbell DJ. T-bet(+) Treg cells undergo abortive Th1 cell differentiation due to impaired expression of IL-12 receptor beta2. Immunity. 2012; 37:501–510. [PubMed: 22960221]

Koch MA, Tucker-Heard G, Perdue NR, Killebrew JR, Urdahl KB, Campbell DJ. The transcription factor T-bet controls regulatory T cell homeostasis and function during type 1 inflammation. Nat Immunol. 2009; 10:595–602. [PubMed: 19412181]

Kubota K. Innate IFN-gamma production by subsets of natural killer cells, natural killer T cells and gammadelta T cells in response to dying bacterial-infected macrophages. Scand J Immunol. 2010; 71:199–209. [PubMed: 20415785]

Nagaraj S, Gabrilovich DI. Tumor escape mechanism governed by myeloid-derived suppressor cells. Cancer Res. 2008; 68:2561–2563. [PubMed: 18413722]

Ostrand-Rosenberg S, Sinha P. Myeloid-derived suppressor cells: linking inflammation and cancer. J Immunol. 2009; 182:4499–4506. [PubMed: 19342621]

Radoja S, Rao TD, Hillman D, Frey AB. Mice bearing late-stage tumors have normal functional systemic T cell responses in vitro and in vivo. J Immunol. 2000; 164:2619–2628. [PubMed: 10679101]

Schoenborn JR, Wilson CB. Regulation of interferon-gamma during innate and adaptive immune responses. Adv Immunol. 2007; 96:41–101. [PubMed: 17981204]

Schreiber RD, Old LJ, Smyth MJ. Cancer immunoediting: integrating immunity's roles in cancer suppression and promotion. Science. 2011; 331:1565–1570. [PubMed: 21436444]

Spranger S, Spaapen RM, Zha Y, Williams J, Meng Y, Ha TT, Gajewski TF. Up-regulation of PD-L1, IDO, and T(regs) in the melanoma tumor microenvironment is driven by CD8(+) T cells. Sci Transl Med. 2013; 5:200ra116.

Swann JB, Vesely MD, Silva A, Sharkey J, Akira S, Schreiber RD, Smyth MJ. Demonstration of inflammation-induced cancer and cancer immunoediting during primary tumorigenesis. Proc Natl Acad Sci U S A. 2008; 105:652–656. [PubMed: 18178624]

Umansky V, Sevko A. Tumor microenvironment and myeloid-derived suppressor cells. Cancer microenvironment : official journal of the International Cancer Microenvironment Society. 2013; 6:169–177. [PubMed: 23242672]

Whiteside TL. The tumor microenvironment and its role in promoting tumor growth. Oncogene. 2008; 27:5904–5912. [PubMed: 18836471]

Wilke CM, Wei S, Wang L, Kryczek I, Kao J, Zou W. Dual biological effects of the cytokines interleukin-10 and interferon-gamma. Cancer Immunol Immunother. 2011; 60:1529–1541. [PubMed: 21918895]

Yu F, Sharma S, Edwards J, Feigenbaum L, Zhu J. Dynamic expression of transcription factors T-bet and GATA-3 by regulatory T cells maintains immunotolerance. Nat Immunol. 2015; 16:197–206. [PubMed: 25501630]

Zaidi MR, Davis S, Noonan FP, Graff-Cherry C, Hawley TS, Walker RL, Feigenbaum L, Fuchs E, Lyakh L, Young HA, et al. Interferon-gamma links ultraviolet radiation to melanomagenesis in mice. Nature. 2011; 469:548–553. [PubMed: 21248750]

Zaidi MR, Merlino G. The two faces of interferon-gamma in cancer. Clin Cancer Res. 2011; 17:6118–6124. [PubMed: 21705455]

Zou Q, Jin J, Hu H, Li HS, Romano S, Xiao Y, Nakaya M, Zhou X, Cheng X, Yang P, et al. USP15 stabilizes MDM2 to mediate cancer-cell survival and inhibit antitumor T cell responses. Nat Immunol. 2014; 15:562–570. [PubMed: 24777531]

Zou W. Immunosuppressive networks in the tumour environment and their therapeutic relevance. Nature reviews Cancer. 2005; 5:263–274. [PubMed: 15776005]

Zou W. Regulatory T cells, tumour immunity and immunotherapy. Nat Rev Immunol. 2006; 6:295–307. [PubMed: 16557261]

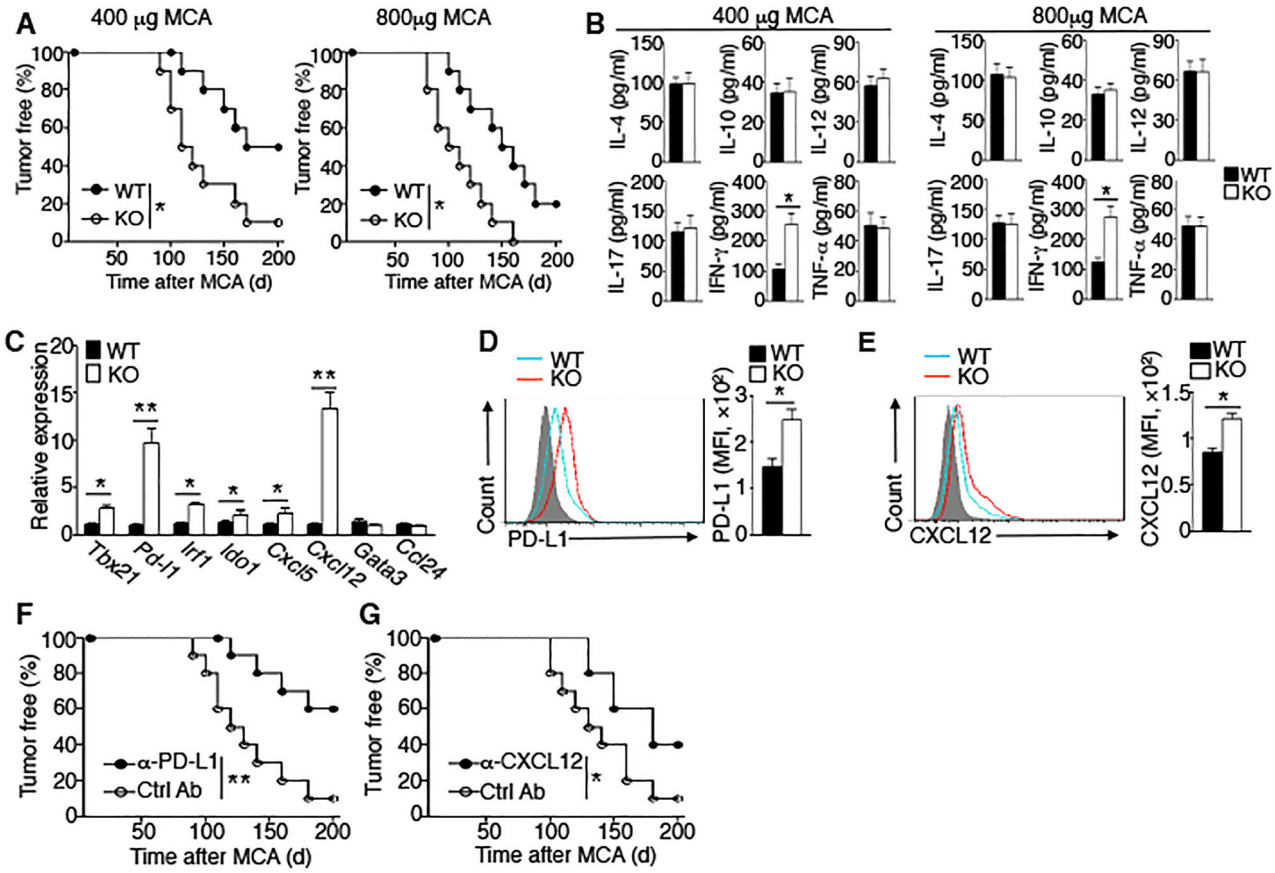

Figure 1. IFN-γ-responsive gene signature in *Usp15*$^{-/-}$ tumor environment

(A) Frequency of tumor-free mice in the wildtype (WT) and *Usp15*$^{-/-}$ (KO) mice injected with two different doses of MCA (400 μg or 800 μg).

(B) ELISA of the indicated cytokines in the serum of wildtype and *Usp15*$^{-/-}$ mice injected with two different doses (400 μg and 800 μg) MCA. The serum was collected from the mice that had developed a palpable tumor (over 25 mm^2) on day 150 after injection of 400 μg or 800 μg MCA.

(C) qRT-PCR analysis of sorted CD45$^-$ cells in the tumor from tumor-bearing wildtype and *Usp15*$^{-/-}$ mice. (D, E) Flow cytometric analysis of PD-L1

(D) and CXCL12 (E) of CD45$^-$ cells in the tumor from tumor-bearing wildtype and *Usp15*$^{-/-}$ mice. Shaded histogram represents isotype control (D, E).

(F, G) Frequency of tumor-free mice in *Usp15*$^{-/-}$ mice treated with either a control antibody (Ctrl Ab) or neutralizing antibodies for PD-L1 (F) and CXCL12 (G) weekly from day 90 to day 146 after injection of 400 μg MCA.

Data are representative of four (A–E) or three (F, G) independent experiments with 10 mice (A, B, F, G) or 5 mice (C–E) per group. Significance was determined by Mantel-Cox test (A, F, G) or two-tailed Student's *t* test (B–E) (*P<0.05; **P<0.01). Data are presented as mean ± SEM. See also Figure S1.

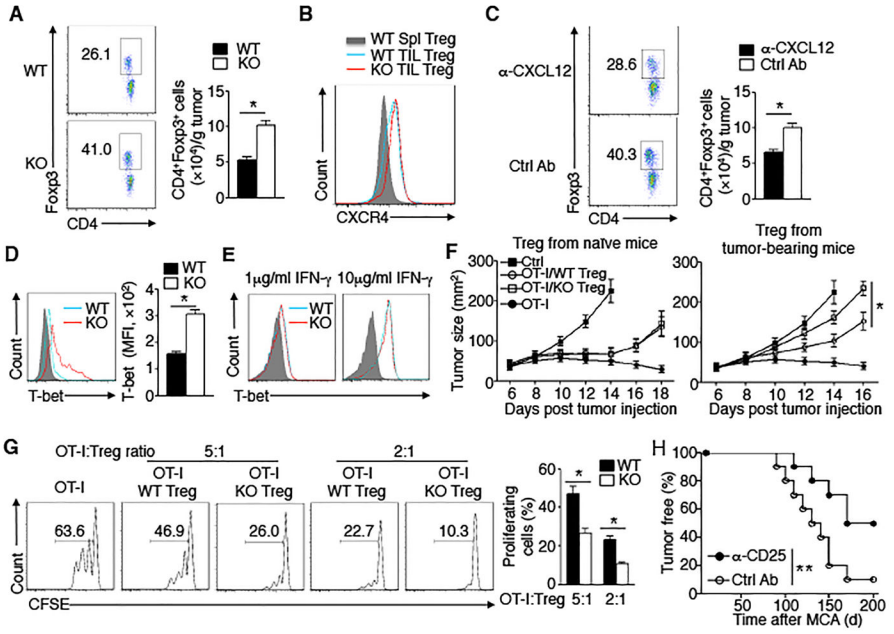

Figure 2. T-bet^{+} regulatory T cells were primed in the tumor-bearing *Usp15*$^{-/-}$ mice

(A) Flow cytometry analysis of Treg cells in TILs from tumor-bearing wildtype (WT) and *Usp15*$^{-/-}$ (KO) mice, showing a representative plot (left) and summary graph of five mice (right).

(B) Flow cytometry analysis of CXCR4 of tumor-infiltrating CD4^{+}Foxp3^{+} cells in the tumor-bearing wildtype and *Usp15*$^{-/-}$ mice. Splenic CD4^{+}Foxp3^{+} cells were used as control (shaded histogram).

(C) Flow cytometry analysis of tumor-infiltrating CD4^{+}Foxp3^{+} cells in the tumor-bearing *Usp15*$^{-/-}$ mice treated with an anti-CXCL12 neutralizing antibody weekly from day 90 to day 146 after injection of 400 μg MCA.

(D) Intracellular T-bet staining of Foxp3^{+}CD4^{+} regulatory T cells in the TILs from tumor-bearing wildtype and *Usp15*$^{-/-}$ mice. Shaded histogram represents isotype control.

(E) Flow cytometric analysis of T-bet expression in CD4^{+}CD25^{+} Treg cells from naïve wildtype and *Usp15*$^{-/-}$ mice stimulated with anti-CD3/anti-CD28 in media containing IL-2 alone (shaded histograms) or IL-2 plus IFN-γ (open histograms) for 4 days.

(F) *Tcrb*$^{-/-}$*Tcrd*$^{-/-}$ mice were injected with 2×10^{5} OVA-expressing B16 cells at day 0. At day 6, mice were treated with PBS control (Ctrl), OT-I T cells, or OT-I T cells plus CD4^{+}CD25^{+} Treg cells sorted from lymph nodes of naïve wildtype (WT) or *Usp15*-KO (KO) mice (left panel), or from draining lymph nodes of tumor-bearing wildtype (WT) or *Usp15*-KO (KO) mice (right panel). Tumor growth was measured every two days. Note that the control group got discontinued on day 14, since their tumors reached the limiting size.

(G) Proliferation assays, based on CFSE dilution, of OT-I T cells in the presence of the indicated ratios of CD4^{+}CD25^{+} Treg cells sorted from tumor-bearing wildtype (WT) or *Usp15*$^{-/-}$ (KO) mice.

(H) Frequency of tumor-free mice in the *Usp15*$^{-/-}$ mice treated with an anti-CD25 neutralizing antibody weekly from day 90 to day 146 after injection of 400 μg MCA.

Data are representative of three independent experiments with 4 mice (A–E, G) or 10 mice (F, H) per group. Significance was determined by Mantel-Cox test (H) or two-tailed Student's *t* test (A, C, D, F, G) (*P<0.05; **P<0.01). Data are presented as mean ± SEM. See also Figure S2.

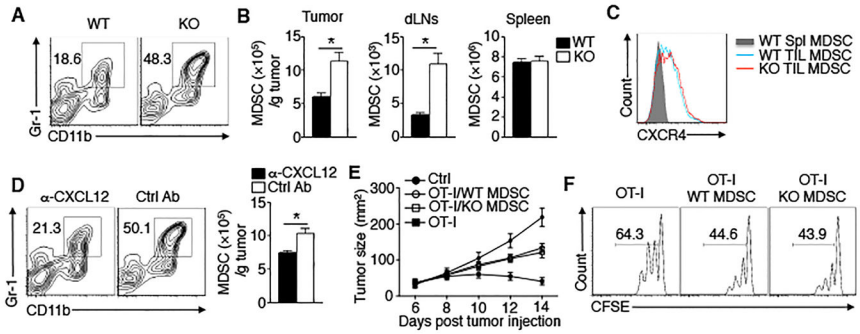

Figure 3. Excessive accumulation of MDSCs in tumor-bearing *Usp15*-KO mice

(A) Flow cytometry analysis of Gr-1$^+$CD11b$^+$ cells in the tumor of tumor-bearing wildtype (WT) and *Usp15*$^{-/-}$ (KO) mice. Data are presented as a representative plot of MDSC frequency.

(B) Summary graph of MDSC absolute numbers in indicated tissues based on five pairs of mice.

(C) Flow cytometry analysis of CXCR4 of tumor-infiltrating Gr-1$^+$CD11b$^+$ cells in the tumor-bearing wildtype and *Usp15*-KO mice. Splenic Gr-1$^+$CD11b$^+$ cells were used as control (shaded histogram).

(D) Flow cytometry analysis of Gr-1$^+$CD11b$^+$ cells in the tumor of the tumor-bearing *Usp15*-KO mice treated with anti-CXCL12 neutralizing antibodies weekly from day 90 to day 146 after injection of 400μg MCA.

(E) *Tcrb*$^{-/-}$*Tcrd*$^{-/-}$ mice were injected with 2×10^5 OVA-expressing B16 cells. On day 6, mice were injected with PBS control (Ctrl), OT-I T cells, or OT-I T cells plus Gr-1$^+$CD11b$^+$ cells sorted from the tumor in the tumor-bearing wildtype and *Usp15*-KO mice. Tumor growth was measured every two days.

(F) Proliferation assays, based on CFSE dilution, of CFSE-labeled OT-I T cells cultured either alone or together with MDSCs (3:1) sorted from tumors of wildtype or *Usp15*-KO mice.

Data are representative of three independent experiments with at least 4 mice per group. Significance was determined by two-tailed Student's *t* test (B, D) (*P<0.05). Data are presented as mean ± SEM. See also Figure S2.

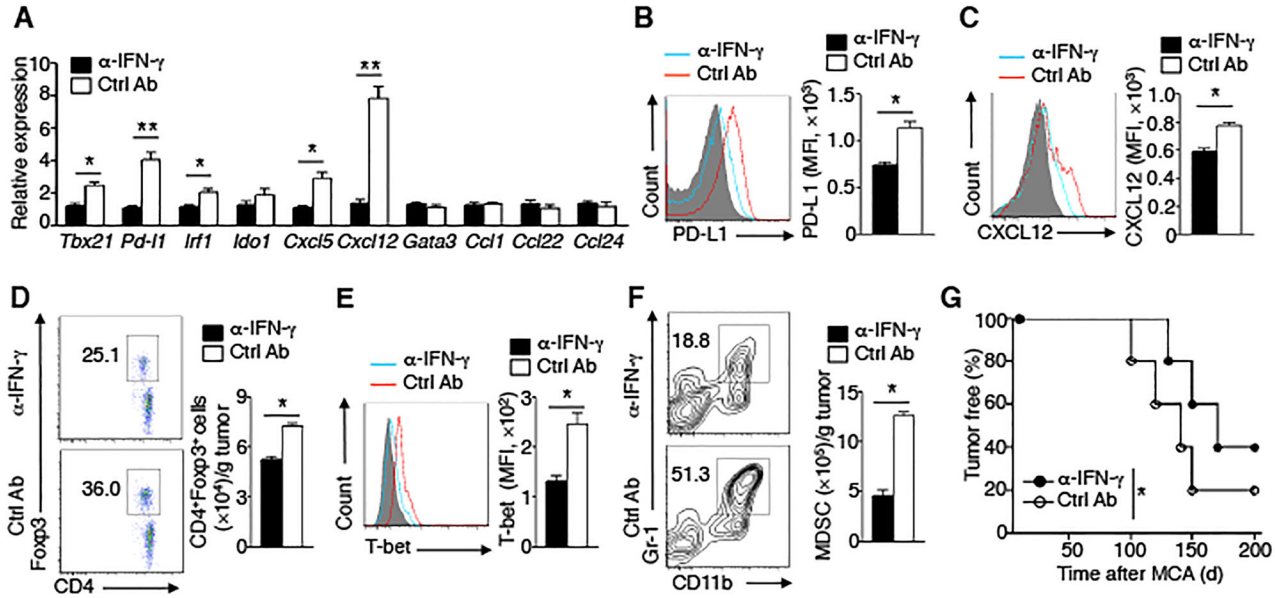

Figure 4. Excessive IFN-γ contributes to the formation of immunosuppressive tumor microenvironment in *Usp15*$^{-/-}$ mice

Tumor-bearing *Usp15*$^{-/-}$ (KO) mice were treated with either a control (Ctrl) IgG1 antibody or an anti-IFN-γ neutralizing antibody weekly from day 90 to day 146 after injection of 400 μg MCA. The treated mice were subjected to the following studies.

(A) qRT-PCR analysis of the indicated genes in sorted CD45^{-} non-immune cells.

(B, C) Flow cytometry analysis of PD-L1 (B) and CXCL12 (C) in CD45^{-} non-immune cells. Shaded histogram represents isotype control (B, C).

(D) Flow cytometry analysis of tumor-infiltrating CD4^{+}Foxp3^{+} Treg cells, presented as a representative plot of Treg frequency (left) and a summary graph of Treg absolute numbers (right).

(E) Intracellular T-bet staining of Foxp3^{+}CD4^{+} Treg cells in the TILs, showing a representative plot (left) and a summary graph of mean fluorescence intensity (MFI, right). Shaded histogram represents isotype control.

(F) Flow cytometry analysis of Gr-1^{+}CD11b^{+} MDSCs in the tumor from antibodies-treated mice.

(G) Frequency of tumor-free mice treated with indicated antibodies after MCA injection. Data are representative of three independent experiments with at least 4 mice (A–F) or 10 mice (G) per group. Significance was determined by Mantel-Cox test (G) or two-tailed Student's *t* test (A–F) (*P<0.05; **P<0.01). Data are presented as mean ± SEM.

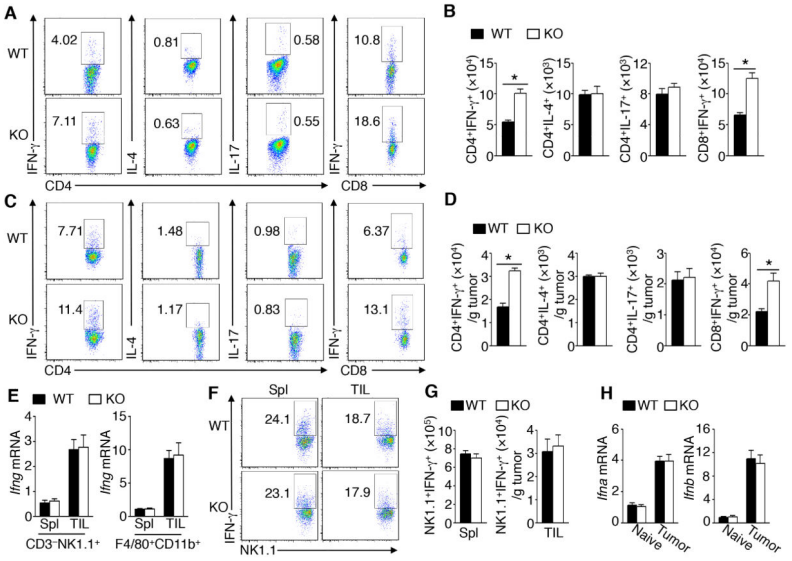

Figure 5. T cells serve as the main source of aberrant IFN-γ in tumor-bearing *Usp15*-KO mice

(A-D) Intracellular staining and flow cytometry analyses of the indicated cytokines in $CD4^+$ or $CD8^+$ T cells from draining lymph node (A, B) or tumor (C, D) of tumor-bearing wildtype (WT) and $Usp15^{-/-}$ (KO) mice. Data are presented as representative plots of cell frequencies (A, C) and summary graph of absolute cell numbers based on five pairs of mice (B, D).

(E) qRT-PCR analysis of *Ifng* mRNA of sorted NK ($CD3^-NK1.1^+$) cells and macrophages ($F4/80^+CD11b^+$) in the spleen (Spl) or TILs of tumor-bearing wildtype and *Usp15*-KO mice.

(F, G) Intracellular staining and flow cytometry analysis of IFN-γ in the splenocytes (Spl) or TILs from tumor-bearing wildtype and $Usp15^{-/-}$ mice treated (i.p.) with 200 μg LPS for 6 h.

(H) qRT-PCR analysis of *Ifna* and *Ifnb* mRNA of DCs ($CD11c^+MHC\text{-}II^+$) sorted from lymph nodes of naïve wildtype and $Usp15^{-/-}$ mice or draining lymph nodes of tumor-bearing (Tumor) wildtype and $Usp15^{-/-}$ mice.

Data are representative of five (A–D) or three (E–H) independent experiments with at least 4 mice per group. Significance was determined by two-tailed Student's *t* test (B, D) (*P<0.05). Data are presented as mean ± SEM. See also Figure S3.

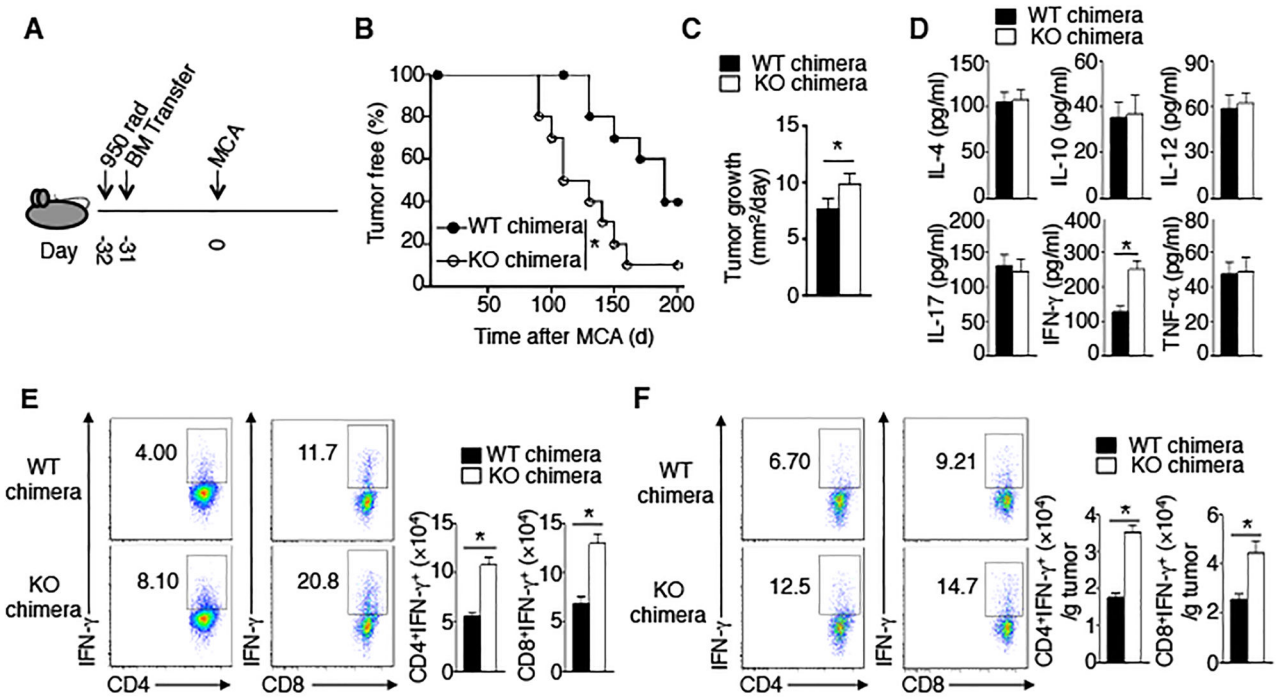

Figure 6. T cell-intrinsic role of USP15 in regulating MCA-induced fibrosarcoma formation

(A) *Usp15*-KO (KO) and wildtype (WT) mixed bone-marrow chimeric mice were generated by adoptive transfer of irradiated *Rag1*-KO mice with $Tcrb^{-/-}Tcrd^{-/-}$ bone marrows mixed (in 4:1 ratio) with bone marrows from *Usp15*-KO and wildtype mice, respectively. The mice were injected with MCA (400 μg) 31 days after bone marrow transfer.

(B) Frequency of tumor-free mice following MCA injection of the WT and *Usp15*-KO bone marrow chimeric mice indicated in panel A.

(C) Tumor growth rates of the chimeric mice from panel B, presented as mm^2/day.

(D) ELISA analysis of the indicated cytokines in the serum collected from the mice described in A with a palpable tumor (over 25 mm^2) on day 150 after MCA injection.

(E, F) Intracellular staining and flow cytometry analyses of IFN-γ in $CD4^+$ and $CD8^+$ T cells isolated from the draining lymph node (E) or TILs (F) of tumor-bearing wildtype and *Usp15*-KO mixed bone marrow chimeric mice described in panel A.

Data are representative of three independent experiments with at least 4 mice (C–F) or 10 mice (B) per group. Significance was determined by Mantel-Cox test (B) or two-tailed Student's *t* test (C-F) (*P<0.05). Data are presented as mean ± SEM. See also Figure S4.

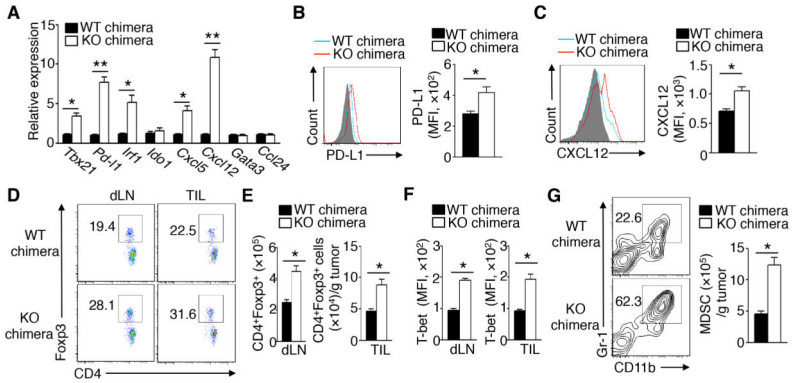

Figure 7. T cell-intrinsic induction of IFN-γ-responsive gene signature in the tumor environment of *Usp15*-KO mice

(A-C) qRT-PCR analysis of the indicated genes (A) and flow cytometry analysis of PD-L1 (B) or CXCL12 (C) in sorted $CD45^-$ non-immune cells from tumor-bearing wildtype and *Usp15*-KO mixed bone marrow chimeric mice described in Fig. 6A. Shaded histogram represents isotype control (B, C).

(D, E) Flow cytometry analysis of Treg cells in the draining lymph node and TILs of the tumor-bearing wildtype and *Usp15*-KO mixed bone marrow chimeric mice described in Fig. 6A.

(F) Intracellular T-bet staining of Treg cells in the draining lymph node (dLN) or TILs of the tumor-bearing wildtype and *Usp15*-KO mixed bone marrow chimeric mice described in Fig. 6A.

(G) Flow cytometry analysis of $Gr\text{-}1^+CD11b^+$ MDSCs in the tumor from the tumor-bearing wildtype and *Usp15*-KO mixed bone marrow chimeric mice described in Fig. 6A.

Data are representative of three independent experiments with at least 4 mice per group. Significance was determined by two-tailed Student's *t* test (A–C, E–G) (*P<0.05; **P<0.01). Data are presented as mean ± SEM. See also Figures S5 and S6.